CHIN. PHYS. LETT. Vol. 33, No. 12 (2016) 124101

Coupling of Cutoff Modes in a Chain of Nonlinear Metallic Nanorods *

Wei-Na Cui(崔维娜)[1,2], Hong-Xia Li(李红霞)[1], Min Sun(孙敏)[1], Yong-Yuan Zhu(朱永元)[2**]

[1]*Department of Applied Physics, Nanjing University of Science and Technology, Nanjing 210094*

[2]*Key Laboratory of Modern Acoustics, National Laboratory of Solid State Microstructures and Collaborative Innovation Center of Advanced Microstructures, Nanjing University, Nanjing 210093*

(Received 4 September 2016)

We study the coupling of cutoff modes in a chain of metallic nanorods embedded in a Kerr nonlinear optical medium with strong near-field interactions analytically. Based on a quasidiscreteness approach, we derive a system of two coupled nonlinear Schrödinger equations governing the evolution of the envelopes of these modes. It is shown that this system supports a variety of subwavelength plasmonic lattice vector solitons of the bright-bright, bright-dark, dark-bright, and dark-dark type through a cross-phase modulation. It is also shown that the existence of different solitons depends strongly on the gap width scaled for the rod radius and the type of nonlinearity of the embedded medium.

PACS: *41.20.Jb, 63.20.Pw, 75.30.Kz, 78.20.Ci* DOI: 10.1088/0256-307X/33/12/124101

Recent progress in nanofabrication of metallic nanostructures has opened novel opportunities for further miniaturization of optical devices. Using surface plasmon of the composite core/shell structures or metallic nanoparticles, one can confine and guide optical energy over distances much smaller than the wavelength.[1,2] The couplings between neighboring elements in metallic nanoparticles generate fascinating physical phenomena, and several theoretical approaches have been successfully established to compute the plasmonic couplings, such as an equivalent LC-circuit model and tight-binding method.[3–6] The coupling interactions can also result in strong local electromagnetic fields, significantly enhancing nonlinear optical processes.[7,8] Moreover, plasmonic excitations are extremely sensitive to the dielectric properties of the metal and the surrounding medium. This extraordinary sensitivity can be exploited to induce an increased effective nonlinear optical response, thus modifying the plasmonic resonances and the signal propagation.[9,10] The subwavelength plasmonic lattice solitons (PLSs) as one of nonlinear excitation has been intensively studied.[11–14] We have recently developed an approach to investigate the subwavelength PLSs in a one-dimensional chain of coupled metallic nanorods.[15] In our case the nanorods are aligned end to end to form a chain and embedded in a Kerr nonlinear optical medium. The subwavelength plasmon bright or dark solitons can be excited by the interplay between discreteness and nonlinearity. However, up to now the study on PLSs are focused on the excitation of a single mode, where it is the self-phase modulation of the carrier wave that has been shown to lead to the generation of nonlinear localized structures. In the following we pay attention to the coupling of two cutoff modes in a nonlinear metallic nanorods chain. There exists a strong interaction between two cutoff different modes not only due to self-phase modulation but also due to cross-phase modulation (CPM),[16] and a novel class of nonlinear localized structures in such a system are expected.

Here we take gold nanorods as the building blocks shown in Fig. 1. In the metallic nanorods chain we are interested in, the nanorods are aligned end-to-end to form a plasmonic waveguide. There is a small gap s between two neighboring nanorods that influences significantly the optical properties of the system. Each nanorod has the length l and the radius r, and the lattice period is $a = l+s$. If the incident light propagates with the electric field along the rod axis, the longitudinal plasmon is supported and the near-field coupling allows electromagnetic energy transport smaller than the diffraction limit. In our model the nanorods chain is assumed to be embedded in a Kerr nonlinear optical medium with an intensity dependence permittivity $\epsilon(|E|^2) = \epsilon_0(\epsilon_1 + \alpha|E|^2/E_c^2)$, where E is the electric component of the applied electromagnetic field, E_c is a characteristic electric field, and $\alpha = +1(\alpha = -1)$ corresponding to self-focusing (-defocusing) nonlinearity. As we know, the coupled LC-resonator scheme is available for the strong coupling effect, then each individual nanorod can be taken as an LC circuit with a field-dependent capacitance. The effective self-inductance is $L = (\mu_0 l/2\pi)ln(l/2r)$ and the capacitance is $C_{10} = \nu\pi\epsilon_0\epsilon_1 r$, where μ_0 is vacuum permeability, ϵ_0 and ϵ_1 represent the vacuum permittivity and linear permittivity respectively, and ν is the fraction of charges distributed on the end faces.[3] It is noticed that there is another effective capacitance $C_{20} = 2\nu\pi\epsilon_0\epsilon_1 r^2/[(r^2+s^2)^{1/2} - s]$ that benefits from the nearest-neighbor nanorods, when the metallic nanorods are aligned in a chain.[4] Considering that the electric field in the capacitive gaps is highly confined near resonance frequencies, the nonlinear properties of the dielectric placed into gaps are enhanced considerably, then nanorods acquire a field-dependent ca-

*Supported by the National Basic Research Program of China under Grant No 2012CB921502, the National Natural Science Foundation of China under Grant Nos 11374150, 11074120, 11274163 and 11274164, and the Priority Academic Program Development of Jiangsu Higher Education Institutions of China.

**Corresponding author. Email: yyzhu@nju.edu.cn

© 2016 Chinese Physical Society and IOP Publishing Ltd

pacitance. It could be expected that if the distance s between two neighboring nanorods is larger, the interaction would be weaker. With only nearest neighbor interactions taken into account, the charge stored in the nth subwavelength nanorod is found to obey the nonlinear evolution equation[15]

$$\frac{d^2q_n}{dt^2}+\gamma\frac{dq_n}{dt}+q_n-\lambda(q_{n+1}+q_{n-1}) -\beta_1 q_n^3-\beta_2(q_{n+1}^3+q_{n-1}^3)=0, \tag{1}$$

with

$$\lambda=\frac{C_{10}}{C_{20}},\ \beta_1=\frac{\alpha}{3\epsilon_1},\ \beta_2=\frac{\alpha}{3\epsilon_1}\frac{\lambda^3}{\delta^2}, \tag{2}$$

where $\delta=s/r$ is the gap width scaled for the rod radius. The loss coefficient γ is usually small ($\gamma\ll 1$) and may account for both Ohmic and radiative losses, which is neglected in the following. The coupling coefficient $\lambda=C_{10}/C_{20}=(\sqrt{1+\delta^2}-\delta)/2$ is always positive, which resulted from the interaction between adjacent sites. It is uniquely determined by the gap width scaled for the rod radius $\delta=s/r$. If one makes the Taylor expansion, it can be approximated by $\lambda\approx(1-\delta)/2$ which exhibits that the coupling effect can be enhanced with decreasing the gap width. The on-site nonlinear term $\beta_1 q_n^3$ describes the self-phase modulation that takes place in the nth nanorod, and the inter-site nonlinear term $\beta_2(q_{n+1}^3+q_{n-1}^3)$ arises from the nearest-neighbor nonlinear interactions. It is shown that the value of β_2 becomes larger and larger with the neighboring nanorods closer, even larger than β_1 due to the huge field amplification in the gap.[15] The signs of β_1 and β_2 are determined by the type of the Kerr medium. If one assumes that q_n varies with the form $\sim\exp i(kna-\omega t)$, the linear plasmon wave along the chain of frequency ω and wave number k is described by the following dispersion relation

$$\omega^2=1-2\lambda\cos ka, \tag{3}$$

where k is the wavenumber. The frequency ω represents the corresponding normalized values ω/ω_0, where the resonance frequency is $\omega_0^{-2}=C_{10}(L+L_{10})$ with the formal inductance L_{10}. Equation (3) shows that there is a lower cut-off frequency $\omega_1=\omega(k=0)=(1-2\lambda)^{1/2}$ and a higher cut-off frequency $\omega_2=\omega(k=\pi/a)=(1+2\lambda)^{1/2}$, which are decided by the parameter λ describing the coupling strength of the system. A schematic presentation of the dispersion relation is shown in Fig. 2. The group velocity can be obtained as $V_{\rm g}=d\omega/dk=\lambda a\sin ka/\omega$. Because the parameter λ is always positive, the group velocity $V_{\rm g}$ is positive and supports forward waves for all $k\in[0,\pi/a]$, while negative, and supports backward waves for $k\in[-\pi/a,0]$. We call the mode $k=0$ with the frequency ω_1 the lower cutoff mode and the mode $k=\pi/a$ with the frequency ω_2 the upper cutoff mode. It is noticed that the two cutoff modes have almost equal (i.e., vanishing) group velocities. If two wavepackets with their wavenumbers of carrier waves centered around $k=0$ or $k=\pi/a$ are excited, they will overlap for a very long time, and the nonlinear interaction between these two wavepackets may be very strong. In the following we will pay attention to the superposition of such two such cutoff modes in this system. The formation of coupled nonlinear localized structures through the CPM is expected.

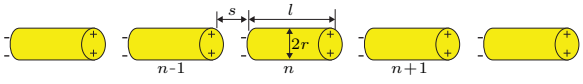

Fig. 1. Schematic view of the subwavelength gold nanorods chain. Each nanorod has radius r and length l embedded in a nonlinear dielectric. The lattice period is $a=l+s$.

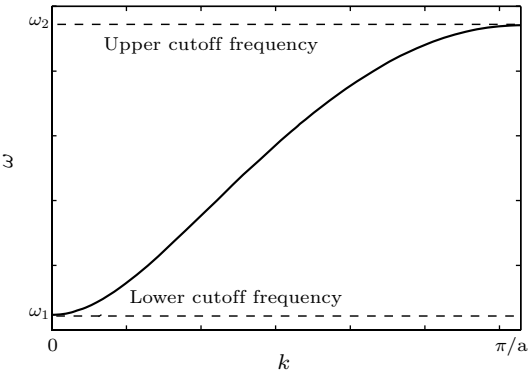

Fig. 2. The linear dispersion relation of the gold nanorods chain. There is a lower cutoff mode $k=0$ with the frequency $\omega=\omega_1$ and an upper cutoff mode $k=\pi/a$ with the frequency $\omega=\omega_2$.

In general, it is impossible to solve analytically nonlinear lattice equations such as Eq. (1). To illustrate the above idea we apply the powerful and clear-cut method called the quasi-discreteness approach, widely used in the nonlinear discrete arrays.[17,18] The basic spirit of the quasidiscreteness approach is the assumption that a linear plane lattice wave is weakly modulated by the nonlinearity of the system. We introduce asymptotic expansion for the charge q_n stored in the nth nanorod as

$$q_n(t)=\sum_{j=1}^{\infty}\varepsilon^j q_{n,n}^{(j)}=\varepsilon q_{n,n}^{(1)}+\varepsilon^2 q_{n,n}^{(2)}+\varepsilon^3 q_{n,n}^{(3)}+\ldots, \tag{4}$$

where ε ($0<\varepsilon\ll 1$) is a small parameter denoting the relative amplitude, and $q_{n,n}^{(j)}=q_{n,n}^{(j)}(\xi_n,\tau;\phi_{1n}(t),\phi_{2n}(t))$ ($j=1,2,3,\ldots$) has two multiple-scale slow variables $\xi_n=\varepsilon(na-V_{\rm g}t)$ and $\tau=\varepsilon^2 t$. The parameter $V_{\rm g}$ is the group velocity, which can also be given by a solvability condition. The fast variables $\phi_{jn}(t)=k_j na-\omega_j t(j=1,2)$ represent the phases of two carrier waves, taken to be completely discrete. The introduction of the multiscale variables means that the derivative expansion is $d/dt=\partial/\partial t-\varepsilon V_{\rm g}\partial/\partial\xi_n+\varepsilon^2\partial/\partial\tau$. Using the above notations, the problem of solving Eq. (1) is converted into a hierarchy of linear but inhomogeneous equations for $q_{n,n}^{(j)}(j=1,2,3,\ldots)$. Since we are interested in two cutoff modes at $k=0$ and $k=\pi/a$, the lowest order solutions with the form of two wavepackets are

assumed,

$$q_{n,n}^{(1)} = A_1(\xi_n,\tau)e^{i\omega_1 t} + A_2(\xi_n,\tau)(-1)^n e^{-i\omega_2 t} + \text{H.c.}, \tag{5}$$

where the first (second) term on the right-hand side corresponds to the lower (upper) cutoff mode, and the two envelope functions A_1 and A_2 are two undetermined functions. The carriers of frequency ω_j and wavenumber $k_j (j = 1, 2)$ satisfy the dispersion relation shown in Eq. (3). The carrier wave is discrete and can be described by a function with the fast variables n and t. The envelope is assumed to be slowly varying in space and time, then A_1 (A_2) is a function of the slow variables ξ_n and τ. Considering that the charge q_n stored in the nth nanorod is real, there is a complex conjugate term in Eq. (1) which is represented by H.c. In the second order, a solvability condition requires $V_g = 0$. In fact, the group velocity $V_g = d\omega/dk = \lambda a \sin ka/\omega$, which vanishes for the cutoff modes. When solving $q_{n,n}^{(3)}$ by two solvability conditions we can obtain the coupled nonlinear Schrödinger (NLS) equations for A_1 and A_2 as follows:

$$\begin{aligned} &i\frac{\partial A_1}{\partial \tau} + \frac{\lambda a^2}{2\omega_1}\frac{\partial^2 A_1}{\partial \xi_n^2} \\ &+ \frac{3(\beta_1 + 2\beta_2)}{2\omega_1}(|A_1|^2 + 2|A_2|^2)A_1 = 0, \end{aligned} \tag{6}$$

$$\begin{aligned} &i\frac{\partial A_2}{\partial \tau} - \frac{\lambda a^2}{2\omega_2}\frac{\partial^2 A_1}{\partial \xi_n^2} \\ &+ \frac{3(\beta_1 - 2\beta_2)}{2\omega_2}(|A_2|^2 + 2|A_1|^2)A_2 = 0. \end{aligned} \tag{7}$$

It is known that the group velocity dispersion coefficient can be calculated as $\omega''(k) = \partial^2\omega/\partial k^2 = (\lambda a^2 \cos ka - V_g^2)/\omega$. We obtain the group velocity dispersion coefficients $\omega''(0) = \lambda a^2/\omega_1$ and $\omega''(\pi/a) = -\lambda a^2/\omega_2$ for the lower and upper cutoff modes, respectively, which results in the different signs of the second-order spatial derivatives in Eqs. (6) and (7). Let $(w, v) = \varepsilon(A_1, A_2)$ and notice $\xi_n = \varepsilon na$ and $\tau = \varepsilon^2 t$, we can rewrite the amplitude Eqs. (6) and (7) in the form

$$i\frac{\partial w}{\partial t} + g_w\frac{\partial^2 w}{\partial x^2} + p_w(|w|^2 + 2|v|^2)w = 0, \tag{8}$$

$$i\frac{\partial v}{\partial t} - g_v\frac{\partial^2 v}{\partial x^2} + p_v(|v|^2 + 2|w|^2)v = 0, \tag{9}$$

with

$$g_w = \frac{\lambda a^2}{2\omega_1},\ g_v = \frac{\lambda a^2}{2\omega_2}, \tag{10}$$

$$p_w = \frac{3(\beta_1 + 2\beta_2)}{2\omega_1} = \frac{1}{2\omega_1}\frac{\alpha}{\epsilon_1}\Big(1 + \frac{2\lambda^3}{\delta^2}\Big), \tag{11}$$

$$p_v = \frac{3(\beta_1 - 2\beta_2)}{2\omega_2} = \frac{1}{2\omega_2}\frac{\alpha}{\epsilon_1}\Big(1 - \frac{2\lambda^3}{\delta^2}\Big). \tag{12}$$

The variable $x = na$ is treated as a continuous one corresponding to the approximation of slowly varying envelopes. We would like to mention that such an approach is commonly used to analyze the nonlinear waves in different kinds of lattice models, such as Refs. [2,3]. The coupled nonlinear Schrödinger Eqs. (8) and (9) have been widely used in many fields and their coupled soliton solutions for some particular coefficients have been derived.[16] However, there are several interesting characteristics of the coupled modes in the nonlinear metallic nanorods chain shown in Eqs. (8) and (9). The first is that the second order derivative terms for w and v with respect to x always have opposite signs due to the positive dispersion coefficients g_v and g_w. The second feature is the nonlinear coefficients p_w and p_v, which may be either sign depending on not only the type of embedded nonlinear dielectric α but also the ratio δ. Lastly, for each mode, in addition to the self-phase modulation term (denoted by $|w|^2 w$ and $|v|^2 v$) there exists a cross-phase modulation term (denoted by $|w|^2 v$ and $|v|^2 w$). As seen from Eqs. (8) and (9), in the absence of CPM coupling the evolution of either the mode w or v is described by a single NLS equation. The modes w and v support bright solitons or dark solitons depending on the embedded nonlinear medium. However, this picture will be changed when the interaction of the lower and upper cutoff modes is considered. Including the cross-phase modulation shown in Eqs. (8) and (9), more types of coupled (vector) solitons can be found in this full version, which are listed in the following.

Due to the interaction of two cutoff modes described by Eqs. (8) and (9) with cross-phase modulation, coupled-mode excitations are possible in the nonlinear metallic nanorods chain. In the following the soliton solutions of the coupled-mode Eqs. (8) and (9) are considered. We derive four types of vector solitons:

(a) Bright-bright solitons in the form

$$w(x,t) = a_1 \text{sech}(bx)\exp(-i\nu_1 t) = f_1\exp(-i\nu_1 t), \tag{13}$$

$$v(x,t) = a_2 \text{sech}(bx)\exp(-i\nu_2 t) = f_2\exp(-i\nu_2 t), \tag{14}$$

with

$$\frac{a_1^2}{b^2} = -\eta_1,\ \frac{a_2^2}{b^2} = \eta_2, \tag{15}$$

$$\nu_1 = -g_w b^2,\ \nu_2 = -g_v b^2, \tag{16}$$

where

$$\eta_1 = \frac{2}{3}\Big(\frac{g_w}{p_w} + 2\frac{g_v}{p_v}\Big),\ \eta_2 = \frac{2}{3}\Big(2\frac{g_w}{p_w} + \frac{g_v}{p_v}\Big). \tag{17}$$

(b) Dark-dark solitons excitations in the form

$$w(x,t) = a_1 \tanh(bx)\exp(-i\nu_1 t) = f_1\exp(-i\nu_1 t), \tag{18}$$

$$v(x,t) = a_2 \tanh(bx)\exp(-i\nu_2 t) = f_2\exp(-i\nu_2 t), \tag{19}$$

with

$$\frac{a_1^2}{b^2} = \eta_1,\ \frac{a_2^2}{b^2} = -\eta_2, \tag{20}$$

$$\nu_1 = -p_w(a_1^2 + 2a_2^2),\ \nu_2 = -p_v(a_2^2 + 2a_1^2). \tag{21}$$

(c) Bright-dark solitons excitations in the form

$$w(x,t) = a_1 \mathrm{sech}(bx)\exp(-i\nu_1 t) = f_1\exp(-i\nu_1 t), \quad (22)$$
$$v(x,t) = a_2 \tanh(bx)\exp(-i\nu_2 t) = f_2\exp(-i\nu_2 t), \quad (23)$$

with

$$\frac{a_1^2}{b^2} = -\eta_1, \ \frac{a_2^2}{b^2} = -\eta_2, \quad (24)$$
$$\nu_1 = -g_w b^2 - 2p_w a_2^2, \ \nu_2 = -p_v a_2^2. \quad (25)$$

(d) Dark-bright solitons in the form

$$w(x,t) = a_1 \tanh(bx)\exp(-i\nu_1 t) = f_1\exp(-i\nu_1 t), \quad (26)$$
$$v(x,t) = a_2 \mathrm{sech}(bx)\exp(-i\nu_2 t) = f_2\exp(-i\nu_2 t), \quad (27)$$

with

$$\frac{a_1^2}{b^2} = \eta_1, \ \frac{a_2^2}{b^2} = \eta_2, \quad (28)$$
$$\nu_1 = -p_w a_1^2, \ \nu_2 = g_v b^2 - 2p_v a_1^2. \quad (29)$$

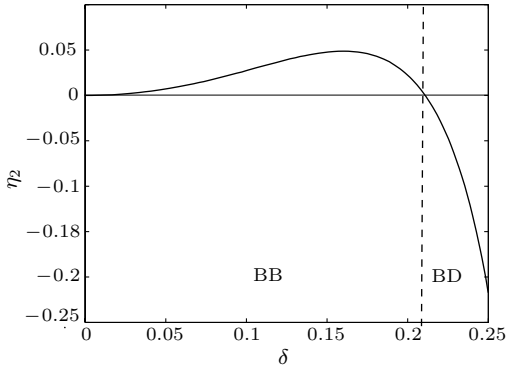

Fig. 3. Dependence of the parameter η_2 on δ corresponding to the self-focusing $\alpha = +1$ and regions for BB and BD solitons.

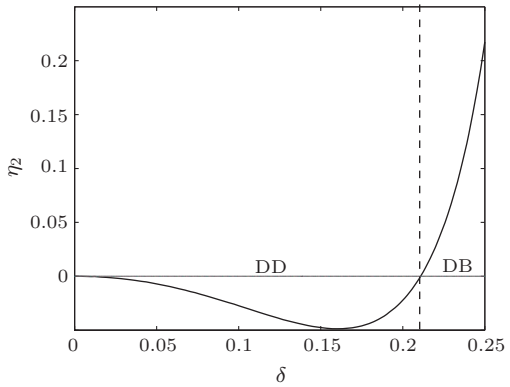

Fig. 4. Dependence of the parameter η_2 on δ corresponding to the self-focusing $\alpha = -1$ and regions for DD and DB solitons.

It is clear that each type of vector soliton is characterized by five parameters a_1, a_2, b, ν_1 and ν_2. The parameters a_j and $\nu_j (j = 1, 2)$ denote the amplitudes and frequencies of each soliton respectively, and the parameter b describes the inverse width of the solitons. Considering that the five parameters are connected by a set of four equations, there is only one free parameter b. On the other hand, the parameters of each soliton component depend on the ones of the other components which are resulted from the nonlinear coupling of the two modes. One can control the characteristics of the lower cut-off soliton by means of the parameters of the higher cut-off pair, and vice versa. The above analytical solutions show that there are four coupled-mode excitations: bright-bright (BB) solitons, dark-dark (DD) solitons, bright-dark (BD) solitons, and dark-bright (DB) solitons. The existence of each type of vector solitons is determined by the signs of parameters $\eta_j (j = 1, 2)$: BB solitons exist for $\eta_1 < 0$ and $\eta_2 > 0$, DD solitons exist for $\eta_1 > 0$ and $\eta_2 < 0$, BD solitons exist for $\eta_1 < 0$ and $\eta_2 < 0$, and DB solitons exist for $\eta_1 > 0$ and $\eta_2 > 0$. The parameters η_1 and η_1 shown in Eq. (17) are dependent on the dispersion coefficient p_j and the nonlinear coefficient g_j $(j = w, v)$ in the coupled NLS Eqs. (8) and (9). It is the parameters δ and α which decide the types of coupled solitons. As we know that the gap width scaled for the rod radius $\delta = s/r$ decreases with the neighboring nanorods closer, in the following the particular interest we have is the extremely small particle separations, i.e., $\delta = s/r < 0.3$, which exhibit strong near-field coupling interaction. The linear permittivity of the nonlinear medium can be taken as $\epsilon_l = 2$. In the case of a self-focusing medium, $\alpha = +1$, η_1 is always negative for $\delta < 0.3$, while η_2 changes the sign at the critical value $\delta = 0.21$, $\eta_2 > 0$ for $\delta < 0.21$, and $\eta_2 < 0$ for $0.21 < \delta < 0.3$, as shown in Fig. 3. Thus one can partition Fig. 3 into two regions concerning $\eta_1 < 0$ and $\eta_2 > 0$ for BB solitons and $\eta_1 < 0$ and $\eta_2 < 0$ for BD solitons. In another case, if the embedded medium is self-defocusing, $\alpha = -1$, the parameter η_2 will just be in the opposite situation, η_2 will be positive in the region $\delta > 0.21$ and negative for $\delta < 0.21$, while the parameter η_1 is always positive. There are also two regions where DD and DB solitons exist respectively as presented in Fig. 4. We can see that the coupled-mode excitations are vector solitons, and they have four types, i.e., bright-bright, dark-dark, bright-dark, dark-bright, corresponding to different parameters regions shown in Fig. 5.

Let us now study the evolution of the coupled solitons presented in the framework of the fully discrete model of Eq. (1). Employing the vector soliton solutions, we can again approximate a solution to Eq. (5) in terms of the original coordinates n and t. The charge stored in the nth subwavelength nanorod for the two-cutoff-mode excitation takes four types as follows: (i) BB soliton solution

$$q_n(t) = 2a_1 \mathrm{sech}(bna)\cos[(\nu_1 + \omega_1)t] + 2(-1)^n a_2 \mathrm{sech}(bna)\cos[(\nu_2 + \omega_2)t], \quad (30)$$

(ii) DD soliton solution

$$q_n(t) = 2a_1 \tanh(bna)\cos[(\nu_1 + \omega_1)t] + 2(-1)^n a_2 \tanh(bna)\cos[(\nu_2 + \omega_2)t], \quad (31)$$

(iii) BD soliton solution

$$q_n(t) = 2a_1 \mathrm{sech}(bna)\cos[(\nu_1+\omega_1)t] + 2(-1)^n a_2 \tanh(bna)\cos[(\nu_2+\omega_2)t], \quad (32)$$

(iv) DB soliton solution

$$q_n(t) = 2a_1 \tanh(bna)\cos[(\nu_1+\omega_1)t] + 2(-1)^n a_2 \mathrm{sech}(bna)\cos[(\nu_2+\omega_2)t]. \quad (33)$$

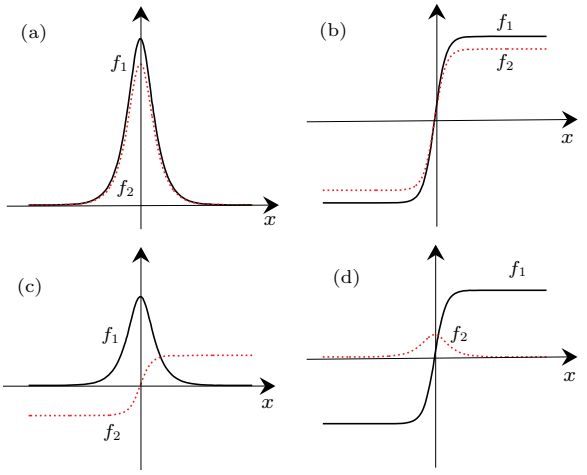

Fig. 5. The patterns of soliton solutions shown in Eqs. (13)–(29) corresponding to the cases (a) BB solitons with $\alpha = +1$, $\delta = 0.1$, (b) DD solitons with $\alpha = -1$, $\delta = 0.1$, (c) BD solitons with $\alpha = +1$, $\delta = 0.23$, and (d) DB solitons with $\alpha = -1$, $\delta = 0.23$.

From the results obtained above we can see that the four types of coupled (vector) solitons exist due to the interaction of the lower and upper cutoff modes exhibited by the CPM effect, which is different from the single-mode excitations. The type of coupled-mode excitations is determined by the embedded nonlinear medium and the gap width scaled for the rod radius. Noticing that in the experimental metallic nanorods array system, one can choose the linear permittivity $\epsilon_1 = 2$ and the nanorods with dimensions similar to those in Ref. [15], i.e., $l = 120\,\mathrm{nm}$, $r = 15\,\mathrm{nm}$ for the nanorod length and radius, respectively. The gap width scaled for the rod radius $\delta = s/r$ has different values with different gap widths s. For example, if one takes $s = 3\,\mathrm{nm}$, then $\delta = 0.2$, which results in BB solitons for a self-focusing medium $\alpha = 1$ and DD solitons for a self-defocusing medium $\alpha = -1$. One obtains the lower cut-off frequency $\omega_1 = 0.42\omega_0$ and a higher cut-off frequency $\omega_2 = 1.35\omega_0$ with the resonance frequency of an isolated nanorod $\omega_0 = 1.84 \times 10^{15}\,\mathrm{rad/s}$. If there is a larger distance between the neighboring nanorods, i.e., $s = 4\,\mathrm{nm}$, then $\delta = 0.26$, BD solitons and DB solitons are possible in different types of embedded nonlinear media as shown in Figs. 3 and 4. Although families of vector solitons were analyzed in the nonlinear case,[16] experimental investigation of nonlinear localized modes in a metallic nanorods chain is currently underway. We hope that our results will provide an alternative way of generating vector solitons, and stimulate much interest in the nonlinear excitations in the subwavelength plasmonic lattice.

In summary, our model is a discrete nonlinear subwavelength metallic nanorods chain where each element is coupled to its nearest neighbors. Based on a quasi-discreteness approach we have derived the nonlinear amplitude equations for two coupled cutoff modes. A novel class of nonlinearly coupled localized structures is possible through a cross-phase modulation. The existence of coupled solitons of the bright-bright, bright-dark, dark-bright and dark-dark types is predicted, which depends on the gap width scaled for the rod radius and the type of embedded medium. Finally, an experiment for observing the coupled nonlinear localized structures in metallic nanorods chain has also been suggested.

References

[1] Atwater H A and Polman A 2010 *Nat. Mater.* **9** 205
[2] Schuller J A, Barnard E S, Cai W, Jun Y C, White J S and Brongersma M L 2010 *Nat. Mater.* **9** 193
[3] Huang C P, Yin X G, Huang H and Zhu Y Y 2009 *Opt. Express* **17** 6407
[4] Huang C P, Yin X G, Kong L B and Zhu Y Y 2010 *J. Phys. Chem. C* **114** 21123
[5] Xi B, Xu H, Xiao S Y and Zhou L 2011 *Phys. Rev. B* **83** 165115
[6] Xi B, Qiu M, Xiao S Y, Xu H and Zhou L 2014 *Phys. Rev. B* **89** 035110
[7] Kauranen M and Zayats A V 2012 *Nat. Photon.* **6** 737
[8] Lapine M, Shadrivov I V and Kivshar Y S 2014 *Rev. Mod. Phys.* **86** 1093
[9] Dickson W et al 2007 *Phys. Rev. B* **76** 115411
[10] Pu Y, Grange R, Hsieh C and Psaltis D 2010 *Phys. Rev. Lett.* **104** 207402
[11] Feigenbaum E and Orenstein M 2007 *Opt. Lett.* **32** 674
[12] Liu Y, Bartal G, Genov D A and Zhang X 2007 *Phys. Rev. Lett.* **99** 153901
[13] Ye F, Mihalache D, Hu B and Panoiu N C 2010 *Phys. Rev. Lett.* **104** 106802
[14] Noskov R E, Belov P A and Kivshar Y S 2012 *Phys. Rev. Lett.* **108** 093901
[15] Cui W N, Zhu Y Y, Huang W X and Li H X 2012 *Phys. Rev. E* **86** 066604
[16] Kivshar Y S and Agrawal G P 2003 *Optical Solitons: From Fibers to Photonic Crystals* (San Diego: Academic)
[17] Huang G P, Tong P Q and Hu B B 1999 *J. Phys.: Condens. Matter* **11** 2759
[18] Cui W N, Zhu Y Y, Li H X and Liu S M 2010 *Phys. Rev. E* **81** 016604